Conformational Changes of Fibrinogen after Adsorption

Matthew L. Clarke, Jie Wang, and Zhan Chen*

Department of Chemistry, University of Michigan, Ann Arbor, Michigan 48109

Received: August 9, 2005; In Final Form: September 21, 2005

The adsorption behavior of fibrinogen to two biomedical polyurethanes and a perfluorinated polymer has been investigated. Changes in the secondary structure of adsorbed fibrinogen were monitored using attenuated total reflection Fourier transform infrared spectroscopy (ATR-FTIR) and sum frequency generation vibrational spectroscopy (SFG). SFG measurements were performed in the amide I range as well as in the C−H/N−H stretching range. Amide I signals from SFG demonstrate that fibrinogen has post-adsorption conformational changes that are dependent upon the polymer surface properties. For example, strong attenuation of the amide I and N−H stretching signals with increasing residence time was observed for fibrinogen adsorbed to poly(ether urethane) but not for the other two polymers. This change is not readily observed by ATR-FTIR. Differences in the observed spectral changes for fibrinogen adsorbed to each polymer are explained by different initial binding mechanisms and post-adsorption conformational changes.

Introduction

Understanding the structural changes of protein molecules after they adsorb to surfaces is of great importance to the development of biomedical materials that have improved biocompatibility.[1−3] The adsorption and resultant structural changes of proteins on foreign materials can ultimately determine whether a material will be accepted by the host system. Despite the significant amount of research that has been performed on protein adsorption, direct details of the molecular changes that occur at surfaces are difficult to obtain due to instrumental constraints. Here, in combination with several more traditional techniques, we apply surface-sensitive vibrational spectroscopy to monitor a single protein, fibrinogen, at several polymer interfaces in situ.

Fibrinogen (∼340 kDa) is a common blood protein and plays a vital role in clot formation. Fibrinogen is of great importance due to its high concentration in the blood, its quick adsorption to foreign materials, and its role in platelet activation and aggregation.[4,5] Several models of the structure of fibrinogen have been developed.[6] For the discussion here, we will consider the structure characterized by a central hydrophobic domain (E domain) connected to two hydrophobic domains (D domains) by coiled coils of α-helices (Figure 1). The connections of the coiled coils are flexible, allowing the protein to bend.[7] The αC chains are connected to each of the D domains and terminate in the αC domains. The αC domains tend to be associated with the E domain[8] but are also known to interact with other αC domains and surfaces.[4]

A number of studies have examined the adsorption of fibrinogen to various polymeric materials using techniques such as radiolabeling, ellipsometry, atomic force microscopy, vibrational spectroscopy, and antibody recognition.[9−16] Using ATR-FTIR, Lenk and co-workers examined fibrinogen structural changes on two different polyurethane surfaces.[17] A change in the relative amounts of secondary structure components was observed with increasing residence time, and these differences were dependent on the polyurethane composition. A study on the adsorption of fibrinogen to several polymers showed that no correlation exists between the amount of fibrinogen adsorbed and the amount of adhered platelets; however a link between antibody recognition of the adsorbed fibrinogen and platelet adhesion was observed.[18] This demonstrates that the adsorbed conformation of fibrinogen is of critical importance, since the conformation determines whether the platelet binding sites will be exposed. In this work, we will show that it is possible to follow the real-time structural changes of adsorbed fibrinogen.

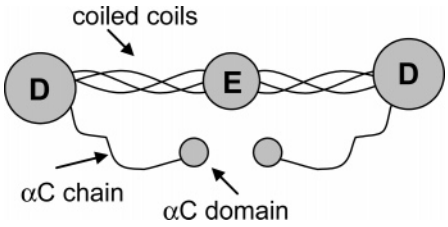

Figure 1. Structure of a fibrinogen molecule with labeled domains.

Obtaining molecular level information about protein conformation at surfaces in situ is an important yet difficult task. Most instrumental methods for protein analysis have limitations such as lack of surface sensitivity, subtraction of large background signals, or requirement of high vacuum. Sum frequency generation (SFG) vibrational spectroscopy is a nonlinear optical technique that has been used recently to study polymer surfaces both in air and in water[19−27] as well as protein and peptide structures at various interfaces.[28−34] In most cases SFG is intrinsically surface-sensitive and can provide information about the presence and orientation of functional groups. The majority of protein analyses by SFG have focused on the protein methyl, methylene, or local water orientation. Only recently have SFG amide I signals from proteins[35,36] and peptides[37,38] been published. Water bending modes should be weak[39] and have not been observed by SFG in the amide I range, simplifying the analysis of the protein vibrational spectrum. The amide I range has been extensively studied by other vibrational spectroscopic techniques, since this range provides information about the secondary structures present in the protein. For example,

* Author to whom correspondence should be addressed. Phone: (734) 615-4189. Fax: (734) 647-4865. E-mail: zhanc@umich.edu.

10.1021/jp054456k CCC: $30.25
Published on Web 10/26/2005

the peak center of the amide I signal of α-helices is around 1650 cm^{-1}, while β-sheet structures have two amide I peaks near 1633 and 1688 cm^{-1}. Turns and random structures each have characteristic amide I signals. Determining which secondary structures exist and their relative orientations will provide the information necessary to understand protein structural changes at surfaces.

Previous research has been performed on fibrinogen using SFG. Jung et al. observed changes in the structure of fibrinogen adsorbed to silica surfaces as a function of pH.[30] Fibrinogen undergoing a pH cycle was bound more tightly to the surface and reacted with a higher amount of antibodies, demonstrating that different parts of the molecule were exposed after the change. A strong SFG N−H stretching signal at 3280 cm^{-1} was observed in the experiment, which was attributed to lysine and arginine side groups on the αC chains. Prior to the pH cycle fibrinogen loosely interacted with the surface via electrostatic interactions with the αC chains. After the cycle the αC chains are displaced, and more of the protein molecule interacts more strongly with the surface. Kim et al. examined the methyl group stretching of fibrinogen adsorbed to hydrophilic silica and hydrophobic polystyrene surfaces using SFG.[31] Results demonstrated that as the concentration of the protein solution increases more methyl groups orient along the surface normal. This indicates that each fibrinogen molecule covers a larger space on the polymer surface when adsorbing from a lower concentration solution (i.e., they have more time to unfold before another fibrinogen molecule adsorbs nearby). It was noted that greater structural changes occur on polystyrene compared to silica.

Polyurethanes are extensively used in biomedical applications, and numerous methods to enhance their biocompatibility have been performed. SFG analysis on polyurethane films shows that the composition of the polymer, including the type of end groups[40,41] or additives such as plasticizers,[42] can have a significant impact on the surface composition of the polymer film. In the present study two biomedical grade polyurethanes were studied: an aliphatic poly(ether urethane) (PEU) and a silicone−poly(carbonate urethane) (SPCU). A perfluorinated polymer (PFP) was also investigated for comparison. In conjunction with the SFG analysis, attenuated total reflection Fourier transform infrared spectroscopy (ATR-FTIR), contact angle goniometry, and quartz crystal microbalance (QCM) measurements are investigated. QCM measurements are included to determine the relative amount of protein that adsorbs to the polymer surface. Comparison of the SFG and ATR-FTIR results illustrates some of the advantages of using SFG to study proteins adsorbed to polymers.

Experimental Section

Reagents. The PEU investigated, Tecoflex SG-80A (Thermedics, Woburn, MA), is an aliphatic poly(ether urethane) synthesized from methylene bis(cyclohexyl) diisocyanate, poly(tetramethylene etherglycol), and chain extender 1,4-butanediol. The SPCU, CarboSil 20 80A (The Polymer Technology Group, Berkeley, CA), is a poly(carbonate urethane) synthesized from hard segment 4,4′-methylene bisphenyl diisocyanate with glycol chain extender and soft segment aliphatic polycarbonate, including poly(dimethylsiloxane) incorporated in the soft segments and as end groups. Fluorinated products AF-40 (1% AF-2400, a copolymer of 2,2-bis(trifluoromethyl)-4,5-difluoro-1,3-dioxole) and FC-40 (fluorinated solvent) were purchased from DuPont (Wilmington, DE). Tetrahydrofuran (THF), toluene, phosphate buffered saline (PBS) (pH 7.4), and bovine fibrinogen were purchased from Sigma-Aldrich (Milwaukee, WI) and used as received.

Sample Preparation. PEU and SPCU were dissolved in THF (2%, w/w). Perfluorinated polymer samples were prepared by mixing equal parts AF-40 and FC-40 by weight. SFG substrates included right-angle fused-silica prisms (for the C−H region) and CaF_2 prisms (for the amide I region). Glass microscope slides were used for contact angle measurements. For QCM measurements, QCM crystals were cleaned by soap and water, soaked and rinsed with THF, and then dried by nitrogen. Crystals coated with PEU or SPCU were adequately cleaned by this method. The AF-2400 coating was not completely removed from the QCM crystals; however, since a given crystal was only used for a particular polymer coating, such a remaining film caused little effect. QCM crystals were replaced as necessary. Fused-silica and glass substrates were cleaned by a sulfuric acid bath saturated with potassium dichromate and thoroughly rinsed with water. CaF_2 prisms and the ZnSe ATR crystal were cleaned using soap, water, and toluene. Polymer films were prepared by spin-coating the polymer solutions at 2000 rpm onto the glass (for contact angle measurements), prism (for SFG measurements), or QCM crystal (for QCM measurements). ATR-FTIR samples were made by solvent-casting a thin film onto the ZnSe ATR crystal. Polymer films made by these methods were optically flat. Fibrinogen solutions of 1 mg/mL were prepared by dissolving fibrinogen in PBS. These solutions were used in experiments within 15 min of their preparation.

Instrumentation. Detailed explanations of the SFG technique have been published before and will not be repeated here.[40,43−47] SFG spectra were collected using an EKSPLA system (Vilnius, Lithuania). Specifics about our system have been described in our previous publications.[19,48] A near total reflection geometry was employed (polymer is coated on a leg face of the prism), which has been previously described.[35] SFG spectra presented in this work were collected using the ssp polarization combination of the input and output laser beams (s-polarized SFG output, s-polarized visible input, and p-polarized IR input). Supplementary ppp spectra were also collected and support the conclusions presented in this paper. The intensity of the ssp SFG signal at a given IR wavelength (ω) can be fitted by

$$I_{ssp}(\omega) \propto \left| \chi_{yyz,nr} + \sum_q \frac{A_{yyz,q}}{\omega - \omega_q + i\Gamma_q} \right|^2 \qquad (1)$$

where $\chi_{yyz,nr}$ is the nonresonant background contribution and $A_{yyz,q}$, ω_q, and Γ_q are the strength, resonant frequency, and damping coefficient of the vibrational mode q, respectively. Spectra were normalized for variations in the visible and IR beam powers. For each type of sample, spectra were collected every 10 min at each interface. In the figures, for each interface, five representative SFG spectra will be shown, and each spectrum is an average of at least three samples. The SFG spectra were found to be very reproducible from sample to sample.

ATR-FTIR spectra were obtained using a Nicolet Magna-IR 550 spectrometer. Spectra collected were averages of 256 scans at 4 cm^{-1} resolution. Spectra of the polymer film in PBS were collected as background spectra and subtracted from spectra obtained after fibrinogen adsorption. The final spectra shown here are difference spectra, and they are averages of three samples. These difference spectra are quite reproducible from sample to sample.

QCM measurements were carried out using a Maxtek Research Quartz Crystal Microbalance (Santa Fe Springs, CA)

TABLE 1: Relative Amount of Fibrinogen Adsorbed to the Polymer Films Determined by QCM as a Ratio Compared to Fibrinogen Adsorbed to PFP at 90 min[a]

	contact angle before fibrinogen adsorption (deg)	fibrinogen adsorption ratio after 90 min	fibrinogen adsorbed after 10 min	percent of fibrinogen rinsed away after 10 min
PEU	70.6	0.79	0.65	15%
SPCU	96.8	0.74	0.56	5%
PFP	125.7	1.00	0.71	1%

[a] Water contact angle measurements of the polymers are also included.

with 10 MHz crystals and a liquid flow cell from Universal Sensors (Metairie, LA). Capacitance cancellation was adjusted in each medium to account for frequency loss due to dissipation in the film or liquid. Details about QCM measurements can be found in the literature.[49−51] Due to the viscoelastic properties of polymers and solutions, QCM studies on these systems require careful consideration. Several studies have employed dissipation monitoring in the QCM system,[52−54] while others have found the ideal linear relationship between the adsorbed mass and the change in frequency (the Sauerbrey equation[55]) to still be appropriate.[56,57] Here, the QCM system was first calibrated by measuring the mass of poly(butyl methacrylate) (PBMA) films of increasing thickness in water. The mass of the PBMA films was calculated from the experimentally determined thickness (using a Dektak Profilometer), the area of the QCM crystal, and the density of PBMA. The mass of adsorbed fibrinogen calculated by using the Sauerbrey equation or the PBMA calibration plot were very similar.

All polymer samples examined by SFG, ATR-FTIR, and QCM were first contacted with PBS for 30 min using a static liquid cell. The buffer solution was then replaced with fibrinogen solution while ensuring the polymer remained wetted in the process. Spectra were then either collected immediately (some SFG C═O measurements), or the fibrinogen solution was kept in contact with the polymer for 10 min and then replaced by PBS, first rinsing with several volumes of PBS (some SFG C═O, all SFG C−H, and all ATR-FTIR measurements). The former considers adsorbed fibrinogen at the polymer/fibrinogen solution interface, and the latter examines adsorbed fibrinogen at the polymer/buffer interface. QCM measurements were taken of fibrinogen adsorption in both of these types of environments.

Static water contact angle measurements of the polymer surfaces were obtained using a CAM 100 Optical Contact Meter (KSV Instruments). Three samples of each polymer were studied, and four contact angle measurements were taken for each of these samples.

Results and Discussion

Polymer Surfaces. Before discussion of the fibrinogen adsorption, it will be informative to examine the surface properties of the polymer films using contact angle goniometry, ATR-FTIR, and SFG. Polymer thicknesses of the PEU, SPCU, and PFP, determined using a Dektak Profilometer, were approximately 100 nm. Polymer thicknesses were not found to significantly affect the ATR-FTIR results. Static water contact angles of the polymer films are shown in Table 1. PEU is the most hydrophilic film, while PFP is the most hydrophobic. This is not surprising as the PEU surface is dominated by the soft segment groups: poly(tetramethylene etherglycol).[42] Contrarily, we expect SPCU and PFP surfaces to be dominated by Si−CH_3 and CF_3/CF_2 groups, respectively.

ATR-FTIR spectra of the polymers in contact with PBS are shown in Figure 2a. These spectra were relatively stable within 10 min after contact, but small changed can be observed in a longer time scale. Both PEU and SPCU films have C═O functional groups in the polymer that are observed by ATR-FTIR, whereas the PFP/buffer interface exhibits only a water bending mode at 1635 cm^{-1}. The water bending signal was also detected from the PEU/PBS and SPCU/PBS interfaces. Detailed analysis of the polymer signals is outside the scope of this paper; however, briefly, peaks corresponding to C═O stretching (1700−1740 cm^{-1}), and N−H bending with C−N stretching (1520−1540 cm^{-1}) are observed for SPCU and PEU, while SPCU has additional peaks at 1590−1615 cm^{-1} from aromatic C−C stretching.[58]

SFG spectra in the C═O stretching range of the three polymers in contact with PBS before fibrinogen adsorption are shown in Figure 2b. PEU exhibits a C═O stretching signal at 1700 cm^{-1}, and SPCU has a signal at 1725 cm^{-1}, while PFP has no signal in this region. This indicates that PEU and SPCU have some oriented C═O groups present at the polymer/PBS interface. Note that polymer C═O signals were also observed at the polymer/air interface for PEU and SPCU at 1715 and 1730 cm^{-1}, respectively. The shift in these peaks upon the polymer contacting buffer indicates that the C═O signals observed are from the polymer/buffer interface rather than the polymer/substrate interface. The C−H SFG spectra of the polymers in PBS are presented in Figure 2c. The C−H stretching signals appear in the wavenumber range between 2700 and 3100 cm^{-1}. Figure 2c also shows the N−H and O−H stretching ranges between 3000 and 3600 cm^{-1}. The PEU and SPCU surfaces have signals originating from the polymer as well as the interfacial water layer, while PFP only exhibits an interfacial water spectrum, because no C−H groups exist in PFP. The PEU surface has main contributions from the soft segment methylene stretching; specifically assignments for major peaks of PEU are: 2850 cm^{-1}, normal CH_2 symmetric stretch; 2920 cm^{-1}, normal CH_2 asymmetric stretch; 2945 cm^{-1}, Fermi resonance. SPCU has a (Si)CH_3 group stretching observed at 2900 cm^{-1} (symmetric) and 2965 cm^{-1} (asymmetric).

ATR-FTIR Results on Fibrinogen. Surface sensitivity of the ATR-FTIR technique is limited by the penetration depth of the infrared beam into the sample. The spectra shown in Figure 2a are contributed by the entire polymer film and some buffer (since the water bending peak can be observed in all three spectra). After the samples have been contacted with fibrinogen solution for 10 min and rinsed with buffer, the fibrinogen amide I and II peaks are readily observed (Figure 3). As mentioned previously in the Instrumentation subsection, Figure 3 shows the difference ATR-FTIR spectra that were obtained by subtracting the spectra collected from the polymer/PBS interface from those collected from adsorbed fibrinogen molecules at the polymer/PBS interface. If we assume that the signals contributed from the polymer film and buffer are the same before and after fibrinogen adsorption, then the difference spectra shown in Figure 3 should only be contributed by adsorbed fibrinogen molecules. However, we will show later that the difference spectra show the signals from adsorbed fibrinogen molecules along with spectral changes of the polymer film or buffer after fibrinogen adsorption. In Figure 3, the peak with a broad feature between 1500 and 1600 cm^{-1} is the amide II signal, while the broad peak between 1600 and 1700 cm^{-1} is the amide I band (Figure 3c). The amide I signal is dominated by the protein backbone C═O stretching modes. The amide II signal has main

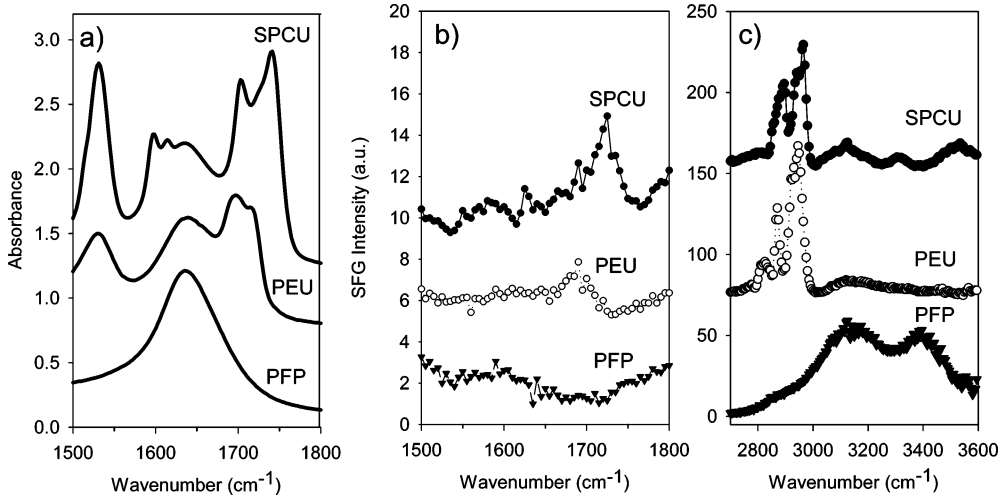

Figure 2. Spectra of SPCU, PEU, and PFP in PBS buffer as detected by (a) ATR-FTIR in the C═O range, (b) SFG in the C═O range, and (c) SFG in the C−H range. Note that the same SFG intensity scale is used for all SFG spectra reported in this research.

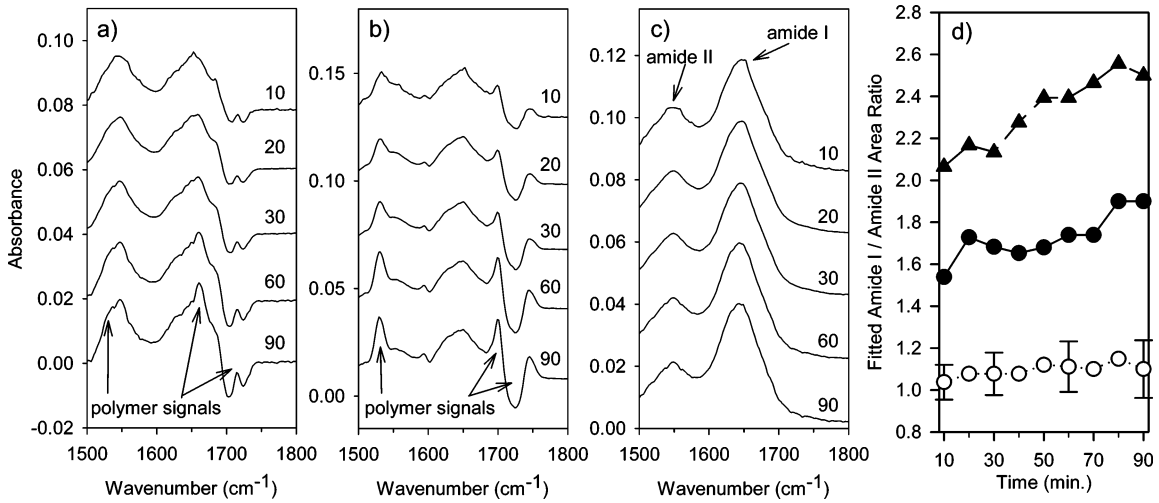

Figure 3. ATR−FTIR spectra of fibrinogen adsorbed to (a) PEU, (b) SPCU, and (c) PFP in PBS buffer in the amide I range collected at different times (in min). Amide I/II area ratio as a function of time (d) from fitting ATR-FTIR spectra for fibrinogen adsorbed to PEU (open circles), SPCU (closed circles), and PFP (closed triangles). Standard deviation is shown for the fibrinogen/PEU sample. Errors for the other samples were similar.

combinations from the backbone N−H bending and C−N stretching modes.

When the basic spectral differences observed for fibrinogen adsorbed onto the three polymer surfaces at any given time are compared, it is noted that the amide I/II area ratio is quite different. To clearly demonstrate this, we fitted the broad features of the amide I and II bands in the ATR-FTIR spectra using a single broad peak for each band. Additional bands were used to account for the narrow signals observed in the PEU/ and SPCU/adsorbed fibrinogen interfaces. The amide I/II area ratio for these interfaces as a function of time is shown in Figure 3d. Fibrinogen adsorbed on PEU exhibits a lower amide I/II area ratio than either SPCU or PFP. All samples exhibit an increase in the amide I/II area ratio with time, with the smallest increase occurring for fibrinogen adsorbed on PEU. Lenk et al. have observed an increased strength of fibrinogen adsorption with an increase in the amide I/II area ratio.[17] These observations may indicate a stronger adsorption of fibrinogen to SPCU or PFP than that to PEU and an increase in fibrinogen adsorption strength with time for all polymer surfaces.

In addition to the broad spectral differences attributed to the amide I and amide II area changes with time, narrow time-dependent peaks are observed in the spectra for fibrinogen adsorbed on PEU and SPCU. There are three possible sources for the appearance and intensity changes of these peaks with time. The first is a result of polymer structure changes, of either the polymer surface or the polymer film bulk, after fibrinogen adsorption. The second source is from structural or orientational changes that occur to the adsorbed fibrinogen molecules. The third is water swelling the polymer film, which could shift or change the intensity of the polymer adsorption bands. It was observed that these changes in the difference spectra on PEU and SPCU have very narrow peak widths (as labeled in Figures 3a and 3b), similar to the widths of the peaks in the spectra collected from polymer/buffer interfaces before protein adsorption (Figure 2a). In addition, such changes have similar peak positions as those in the spectra shown in Figure 2a. We believe that such spectral changes are caused by shifts in the polymer C═O modes as a result of water diffusion into the polymer film. Very small spectral changes in the ATR-FTIR spectra of the polymer/PBS interfaces with time can be observed, and these small changes can be on the order of the fibrinogen amide signals. Again, the difference ATR-FTIR spectra shown in Figure 3 measure the signals of adsorbed fibrinogen and signal differences of the entire polymer film during the time course of the experiment. According to the peak width and peak center argument above, we believe that the narrow spectral changes are dominated by spectral changes of the polymer film rather

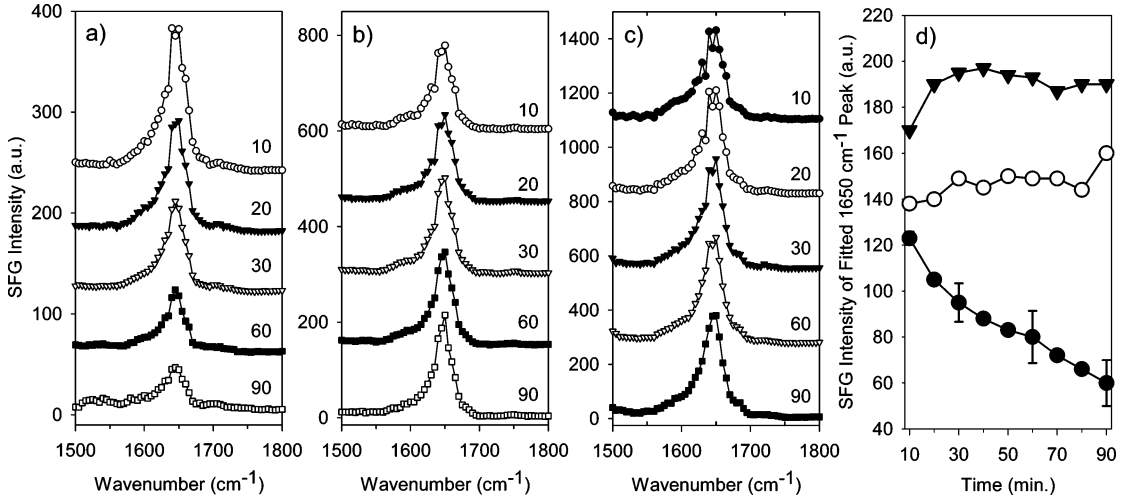

Figure 4. SFG spectra of fibrinogen adsorbed to (a) PEU, (b) SPCU, and (c) PFP in PBS buffer in the amide I range collected at different times (in min). α-Helix SFG signal as a function of time (d) from fitting SFG spectra for fibrinogen adsorbed to PEU (closed circles), SPCU (open circles), and PFP (closed triangles). Representative error is shown for the fibrinogen/PEU sample.

than adsorbed fibrinogen. The broad bands in Figure 3 are contributed by the amide signals of adsorbed fibrinogen molecules.

From the above analysis of the ATR-FTIR amide I band, even though small spectral changes were observed, such changes in spectral features and intensities were not significant. This indicates that no large denaturing of the fibrinogen molecules takes place on these surfaces and that there are not significant changes in the relative amounts of the secondary structures present (e.g., changes from α-helices to β-sheets) during the time scale of our experiment. Additional ATR-FTIR experiments (not shown), performed by adsorbing known amounts of fibrinogen to the polymer surfaces and comparing these results to those in Figure 3, indicate that roughly a monolayer of fibrinogen exists on the polymer films under the conditions reported here.

QCM Measurements. Two types of QCM measurements were performed. In the first case, fibrinogen was allowed to adsorb to a polymer film for 90 min. For the second case, only 10 min were allowed for adsorption. In both experiments, the sample cell was then flushed with PBS. Results from the QCM studies are shown in Table 1. The amount of fibrinogen adsorbed includes both the strongly and the loosely bound protein. The percent of the fibrinogen rinsed away (loosely bound) was calculated based on the mass of adsorbed fibrinogen before and after rinsing with PBS. Both PEU and SPCU have similar fibrinogen adsorption amounts despite their large difference in hydrophobicity. Though PEU adsorbs slightly more fibrinogen, more of this fibrinogen is loosely bound and can be removed by rinsing with PBS than the fibrinogen on SPCU. PFP adsorbs the most fibrinogen with the least amount of loosely bound fibrinogen. This supports the ATR-FTIR result based on the amide I/II area ratio observed. AFM studies (unpublished results) of PEU, SPCU, and PFP indicate that all surfaces are relatively flat; therefore the differences in fibrinogen adsorption amounts are not caused by differences in surface area. The QCM results also indicate that the surface coverage of fibrinogen on both PEU and SPCU surfaces should be approximately equal, while PFP will have a slightly higher coverage of fibrinogen.

It should be noted that the absolute value for the protein adsorption amount cannot be easily determined by this method. Differences in the amount of water within the adsorbed protein film can alter the QCM measurement.[52,54] However, we expect that, though the relative amount of water within the protein film may depend on the polymer involved, the data shown in Table 1 can still give a qualitative value for the relative amount of fibrinogen present at each surface.

SFG C═O Signals. As previously mentioned, two types of SFG samples were considered. In the first case the fibrinogen solution remains in contact with the polymer film for only 10 min before being replaced with buffer. Spectra taken from such samples detect the amide I modes from fibrinogen at the polymer/buffer interface. In the other case fibrinogen solution remains in contact with the surface, and the spectra taken are from the polymer/protein solution interface. Though signals from the polymer surface (Figure 2b) may interfere in the collection of amide I spectra, we believe that this interference is minimal, because the intensities of the SFG polymer C═O signals are much weaker than that observed for the fibrinogen amide I SFG signal and the peak centers are different, allowing the polymer signals to be easily separated by spectral fitting.

SFG spectra collected from fibrinogen adsorbed to all three polymer surfaces contain similar spectral features (Figures 4a−c). All of the spectra were fitted using eq 1, based on parameters from a previously published ATR-FTIR analysis of fibrinogen.[17,59] The spectral fitting components for the SFG spectra collected at 10 and 90 min after fibrinogen adsorption for each polymer are shown in Figure 5 as examples of the fitting quality. See the Supporting Information for more details. Differences between these spectra can be found by detailed spectral fitting and will be discussed shortly; however, the basic spectral components will be mentioned presently. Spectral fitting results indicate that the dominant peak observed in the amide I SFG spectra is located at 1650 cm^{-1}, which is indicative of α-helix components. Other major secondary structures observed in the spectral fitting in decreasing intensity order are intramolecular β-sheet (1635 cm^{-1}) and turn structures (1668 cm^{-1}). Since fibrinogen has a large amount of α-helices it is not surprising that the α-helix signal is dominant. The majority of the α-helix components in fibrinogen can be found in the two coiled coils, and we believe that the SFG signals are mainly contributed by these coiled coils. Small amounts of α-helix components in other domains of fibrinogen cannot generate such strong SFG signals. However, the number of α-helices in a protein is not an indicator of SFG α-helix signal intensity. In other research we found that albumin, which has a large number of α-helices but with little net orientation, has a very weak SFG amide I signal.[35] The ordering of the α-helices into the coiled coils in fibrinogen

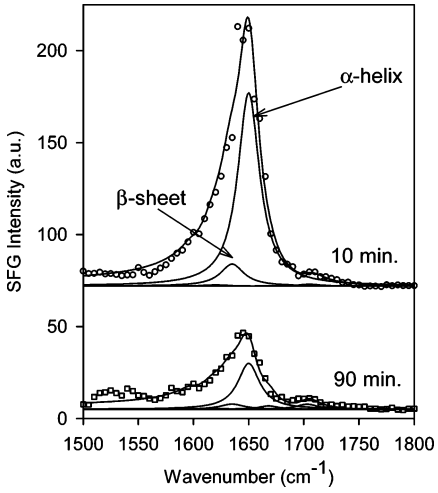

Figure 5. Fitted SFG spectra of fibrinogen adsorbed to PEU in PBS buffer in the amide I range collected at 10 and 90 min. Experimental data shown as points with the fitting results shown as lines. The component peaks of the fitting results are also shown as lines.

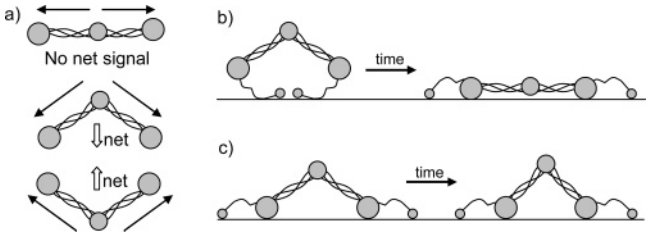

Figure 6. (a) A few of the possible configurations of fibrinogen at the interface. The α-helix signal from each set of coiled coils is shown by solid arrows, and the net α-helix SFG signal is shown by white arrows. αC chains are not shown. (b) Schematic of fibrinogen structural changes with time after adsorption on PEU. (c) Schematic of fibrinogen structural changes with time after adsorption on SPCU or PFP.

allows for large net orientation to occur and therefore strong SFG signals. The net dipole of an α-helix is from the N-terminus to the C-terminus. In the case of fibrinogen this is from the E domain to the D domain. The ssp geometry employed in this study is sensitive to functional groups that have an orientation perpendicular to the sample surface. Since SFG signal will only be from the adsorbed film, if it lacks overall inversion symmetry, then we can conclude that the signal observed from adsorbed fibrinogen is a result of bent conformations. No α-helical signal from the pair of coiled coils would be detected if fibrinogen laid down completely on the surface. If the molecule was in a linear conformation, no matter whether it stood up or tilted on the surface, then no signal would be observed, because the net dipole of the α-helical modes from the pair of coiled coils would cancel. Figure 6 shows some of the possible conformations of fibrinogen at the interface and the resulting net α-helix signal.

Figure 4a shows that fibrinogen adsorbed on PEU exhibits a time-dependent decrease in the amide I signal. Additional experiments show that this decrease is not caused by laser irradiation effects (Supporting Information). Spectral fitting indicates that the reduction in signal principally results from the reduction in the α-helix signal. The fitted spectral intensities of the 1650 cm^{-1} peak collected from fibrinogen adsorbed on all three polymers were plotted as a function of time in Figure 4d. It is observed that the intensity of the 1650 cm^{-1} α-helix peak from the SPCU/ and PFP/adsorbed fibrinogen interface initially increases slightly and then remains relatively stable with time. However, the α-helix signal decreases with time at the PEU/adsorbed fibrinogen interface.

In addition to the major α-helical component change, changes of other secondary structures of adsorbed fibrinogen on PEU have also been observed. An increase in the number of turn structures is observed by the increase in the signal at 1668 cm^{-1}, while the number of β-sheet structures decreases slightly, as shown by the intensity decrease of the 1635 cm^{-1} peak in the fitting. The signal attenuation could be caused by a change in the concentration or orientation (or both) of fibrinogen molecules at the surface. On the basis of the ATR-FTIR and QCM data, we can conclude that after 10 min in contact with the protein solution there are no large changes in the amount of fibrinogen on the polymer surface. Additionally, the ATR-FTIR spectra indicate that no significant loss of fibrinogen secondary structure or significant conversion among different secondary structures occurs with increased residence time on the polymer surface. Therefore, the decrease in the SFG signal indicates that a change in the orientation of the protein secondary structure is occurring rather than a loss of secondary structure or conversion between different secondary structures. The reduction in the α-helix signal is most probably caused by a change in the angle between the coiled coils (larger angles would reduce the SFG signal intensity). The initial conformation of fibrinogen as it adsorbs to the PEU surface is not the lowest energy state. With time the fibrinogen molecules change conformation to increase favorable interactions with the substrate and other adsorbed fibrinogen molecules. A schematic of the time-dependent change of fibrinogen after adsorption on PEU is shown in Figure 6b. The initial binding of fibrinogen by the αC chains will be discussed in the next section.

However, fibrinogen adsorbed to SPCU or PFP exhibits different behavior. The amide I intensity appears to increase with the hydrophobicity of the polymer film: PEU < SPCU < PFP. The amide I signal from the SPCU/fibrinogen interface remains nearly constant over the 90 min observation time, while the signal from the PFP/fibrinogen interface increases. Spectral fitting indicates that the increase in SFG signal from fibrinogen adsorbed to PFP is mainly a result of an increase in the α-helix structural components, as shown in Figure 4d, with some small increase observed for intramolecular β-sheets. These results suggest that a slight narrowing of the angle between the coiled coils occurs for fibrinogen adsorbed on PFP. This implies that the initial adsorbed state and subsequent conformational changes of fibrinogen on PEU and PFP are different. A possible schematic of fibrinogen structural changes after adsorption on PFP and SPCU is shown in Figure 6c. The fibrinogen is shown to interact with the surface by the D domains, which are surface-active and likely to interact with hydrophobic surfaces.[4]

To compare the differences between systems where the fibrinogen solution remains in contact with the polymer to cases where the liquid cell is flushed with buffer, an example of PEU in both situations was monitored. In each case the amide I signal from the absorbed fibrinogen decreases with time. This indicates that the loss in signal is not simply due to increased fibrinogen adsorption causing inversion symmetry in the film probed by SFG because in the buffer case no increased fibrinogen adsorption at the interface can occur. However, there are some differences in the rate of the amide I attenuation. At 10 min, the fibrinogen solution/PEU interface exhibits a stronger amide I intensity than the PBS buffer adsorbed fibrinogen/PEU interface. After 90 min, both PEU systems have approximately the same SFG intensity at 1650 cm^{-1}. The fibrinogen signal decreases at a faster rate when the protein solution remains in contact than if it is replaced with buffer. We believe that this is a result of protein−protein interactions. When protein solution

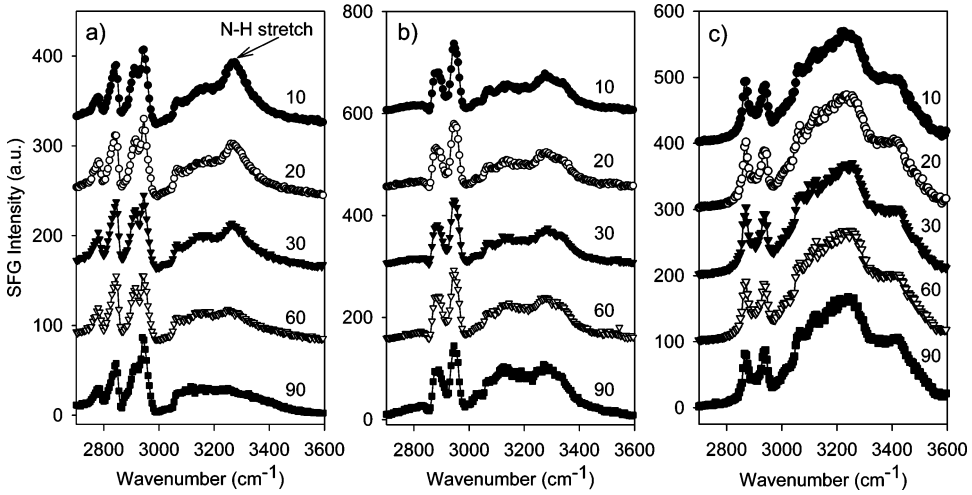

Figure 7. SFG spectra of fibrinogen solution contacting (a) PEU, (b) SPCU, and (c) PFP in the C−H range collected at different times (in min).

remains in contact, then the amount of protein adsorbed at the interface might be greater. Possibly, interactions with neighboring proteins allow for a faster transition from the initially adsorbed state to a more strongly adsorbed state. When protein solution is replaced with buffer, then there are fewer fibrinogen molecules to adsorb (hence the smaller initial SFG signal), and the process requires more time.

At this stage we want to further discuss what different structural information can be deduced from ATR-FTIR and SFG spectra. As mentioned, the surface sensitivity of ATR-FTIR is determined by the penetration depth of the infrared beam; therefore in this experiment, it detected signals from the entire polymer, adsorbed protein, and some buffer. To deduce the structure of adsorbed fibrinogen, we need to use the difference spectra, which exclude the contribution of the polymer bulk and buffer. However, ATR-FTIR protein signals can have interference from the structural changes of the bulk polymer or buffer, as we encountered in Figure 3. In addition, ATR-FTIR is an incoherent spectroscopy; even though polarized ATR-FTIR can provide information about functional group orientation (by measuring average $\cos^2 \theta$, where θ is the angle of a functional group versus the surface normal), such a measurement is not as sensitive as SFG (which measures average $\cos \theta$ and $\cos^3 \theta$). Therefore, the ATR-FTIR spectra may not be very different even if the protein adopts different conformations (e.g., different relative orientations of the two coiled coils as shown in Figure 6a). However, different secondary structures such as α-helices, β-sheets, turns, or random coils contribute to ATR-FTIR amide signals at different wavenumbers. Therefore, similar time-dependent ATR-FTIR spectra of adsorbed fibrinogen shown in Figure 3 indicate that no substantial structural changes of adsorbed fibrinogen occurred (e.g., no large conversion among different secondary structures in fibrinogen); otherwise the spectra features should noticeably change.

SFG is a coherent spectroscopic technique that can selectively detect vibrational spectra from the adsorbed fibrinogen film with no contribution from the bulk polymer and PBS buffer. Thus we do not need to subtract the background to deduce SFG spectra contributed by adsorbed fibrinogen and avoid any error associated with background subtraction. It should be emphasized that the SFG signals detected are from the net orientation of proteins in the entire adsorbed film rather than just from functional groups close to the polymer surface.[60] The coherent nature determines that SFG is very sensitive to the orientation of the functional groups. If the molecule adopts the linear conformation shown in Figure 6a, then no signal can be detected. On the contrary, the bent conformation of fibrinogen can contribute SFG signal. More quantitatively, SFG signal intensity is related to the angle between the two coiled coils in a fibrinogen molecule. Quantitative determination of time-dependent bent structural change after fibrinogen adsorbed on a surface is under current study and will be reported in the future. In this research, we demonstrated clearly that SFG can provide structural information of interfacial protein, which is difficult to probe using only ATR-FTIR.

SFG C−H, O−H, and N−H Signals. As mentioned in the Introduction, SFG research has been focused on the study of C−H groups to deduce structures of surfaces and interfaces. Here we want to show that for interfacial protein molecules, from SFG C−H signals, some structural information can be deduced, but such structural information is not as abundant as that obtained from SFG amide signals. In this research, SFG spectra were collected in the C−H stretching region. Spectra obtained from the polymer/protein solution interface as functions of time are displayed in Figure 7. It is quite difficult to interpret the changes in the C−H stretching region for PEU and SPCU due to the spectral interference of the polymer and protein signals. However, the C−H stretching modes of fibrinogen adsorbed on PFP can be discussed. Fibrinogen adsorbed on PFP exhibits a methyl symmetric stretch at 2870 cm^{-1} and Fermi resonance/asymmetric stretch at 2940 cm^{-1}. Spectral changes with time are small, but reduction in the symmetric stretch intensity can be observed. This reduction must be due to the structural changes of fibrinogen after adsorption, but it is difficult to deduce such structural changes from C−H stretching signal changes. As we revealed by our SFG C═O studies above, the angle between two coiled coils decreased after adsorption as a function of time.

Figure 7 shows that the SFG O−H signals have broad bands mainly covering the spectral range between 3000 and 3600 cm^{-1}. When the O−H stretching region of the spectra in Figure 7 is examined, it is observed that water molecules have a greater alignment on the PFP surface (Figure 7c). The intensities of the O−H stretching modes at the PFP with the adsorbed fibrinogen/PBS solution interface remain nearly identical over time, implying that no restructuring of the water layer occurs. The interfacial water signals from the SPCU/fibrinogen solution interface are stable for approximately 40 min and then increase with time. Our SFG amide I signals collected from the SPCU/fibrinogen solution interface indicate almost no structural changes of fibrinogen after adsorption (Figure 4b); thus such water signal changes might be due to their orientation change

induced by small changes of the SPCU surface structures. At the PEU/fibrinogen interface there is some reduction in the interfacial water signal. The change in the water signal indicates that as fibrinogen undergoes structural changes after adsorption on PEU, as indicated by the changes in the amide I signal shown in Figure 4a, interfacial water molecules must change their orientations. Fibrinogen adsorbed on PEU also exhibits an N−H stretching peak (which is much narrower than the O−H bands) at 3275 cm^{-1} that decreases with time. Comparing the N−H peak in Figure 7 to the C═O peak in Figure 4, we see similar time-dependent trends, though the peak at 3275 cm^{-1} includes signal from water modes. Time-dependent studies of fibrinogen on PEU monitoring the 3275 and 1650 cm^{-1} peaks show a strong correlation (Supporting Information). N−H stretching peaks from fibrinogen adsorbed on SPCU are weaker and do not change with time. Such time-independent SFG N−H signals correlate well to the time-independent SFG amide I signals. The similar time-dependent SFG amide I and N−H signal changes (or lack of change) of fibrinogen adsorbed on PEU and SPCU indicate that possibly the N−H signals are contributed from backbone N−H groups, but we cannot exclude the possibility that side chains can contribute substantial SFG N−H signals, as demonstrated in the literature.[30] SFG spectra in the N−H stretching range from the fibrinogen/PFP interface are more difficult to interpret, due to the interference of the large water signals that can be difficult to analyze.[61] Spectral fitting indicates that there are N−H stretching signals from this interface. However, these signals are much broader than those observed from the fibrinogen/PEU interface. When we compare the amide I/N−H stretching intensity ratio for fibrinogen absorbed at the three interfaces, large differences were found. This suggests that the N−H signal may be contributed by both backbone and side chains. The similar time-dependent behavior of SFG N−H and amide I signals of fibrinogen after adsorption may indicate that N−H signals are dominated by backbone N−H groups. It also may indicate that N−H signals can be dominated by side chain contributions, and such side chains have a similar time-dependent change as the protein backbone conformation changes after adsorption. The following mechanism of adsorbed fibrinogen structural changes attributes the N−H signal changes predominantly to side chain changes.

The large intensity of the N−H stretching peak at 3275 cm^{-1} for fibrinogen adsorbed to PEU compared to that of SPCU or PFP is likely a result of a different initial adsorption conformation of the fibrinogen molecule. This signal could have significant contributions from the side chain lysine and arginine groups on the αC chains of fibrinogen.[30] Likely, the αC chains are able to quickly but loosely bind to the PEU hydrophilic surface (Figure 6b), resulting in ordered N−H groups. Similar binding mechanisms for fibrinogen have been suggested previously.[4] However, this is not the most stable conformation for the adsorbed protein, and with time the backbone structure of the fibrinogen molecule reorients; the αC chains now may interact with other domains intra- or intermolecularly. This results in reduced order for the fibrinogen lysine and arginine groups along the surface normal, causing the observed attenuation of the SFG N−H stretching signal. Since this structural change is linked to the backbone conformation change, we observe a correlation between the decrease in the amide I and N−H stretching signals. Since the spectral features and time-dependent changes for fibrinogen adsorbed on SPCU or PFP are different from that of PEU, we conclude that fibrinogen has a different initial adsorption state on PEU than that on SPCU or PFP. The subsequent conformational change of fibrinogen on PEU will therefore also be unique, and as seen by the amide I SFG spectra, the adsorbed conformation of fibrinogen on PEU after 90 min must be quite different from that on SPCU or PFP. Fibrinogen adsorbed to SPCU and PFP has stronger interactions with these polymer surfaces as indicated by the QCM results. With this stronger initial binding, substantial conformational change of the adsorbed protein is either not favorable or inhibited. The small increase in the fibrinogen α-helix signal may be due to the narrowing of the angle between the two coiled coils (Figure 6c).

Recent SFG studies of fibrinogen adsorbed to polystyrene demonstrate that the fibrinogen amide I band decreases with time but not as fast as fibrinogen on PEU.[62] This shows that other surface−protein interactions are also possible. As mentioned, the quantitative relationship between SFG spectra of an α-helical component, especially spectra collected with different polarization combinations, and the orientation of α-helices on the surface is under current investigation and will be reported soon. Such a relationship will help us to quantify the time-dependent angles between the coiled coils of fibrinogen adsorbed on polymer surfaces in the future.

Conclusion

Investigation of fibrinogen adsorption by SFG, ATR-FTIR, and QCM has shown that fibrinogen binds and undergoes conformational changes that are highly dependent on the chemical properties of the surface. Fibrinogen interactions with SPCU and PFP surfaces appear to be quite favorable, and few structural changes were observed. Initial binding mechanisms for fibrinogen on PEU likely involve the αC chains, which subsequently reorient along with the backbone of the fibrinogen structure to form more favorable interactions with the polymer surface. The SFG signal from the amide I and N−H stretching peaks decrease as a larger proportion of the bound fibrinogen change from the loosely to the more strongly bound states. Fibrinogen adsorbs to SPCU and PFP in a stronger bound state, and only slight changes in the protein conformation are observed with increased adsorption time.

These post-adsorption changes are most readily observed by the SFG technique. Shifts in the polymer C═O vibrational modes due to changes in the hydrogen bonding states of the polyurethane surfaces with fibrinogen compared with PBS interfere with the analysis of the amide I region of the ATR-FTIR spectra. SFG analysis is simplified because no large background subtraction is needed and the polymer C═O SFG signals are much weaker compared to the fibrinogen amide I spectral features. These advantages and the work shown here support the use of SFG to study proteins at surfaces, including monitoring real-time structural changes in situ.

The molecular interactions between polymer surfaces and protein molecules determine the biocompatibility of these polymers. Future studies will seek to combine spectroscopic information with biochemical methods so that the correlations between protein adsorption and the biocompatibility of biomaterials can be understood in detail.

Acknowledgment. The authors thank William Steinecker for his help starting the QCM measurements. This work is supported by the Beckman Foundation and Office of Naval Research. We thank the Polymer Technology Group, Inc. for providing the SPCU samples.

Supporting Information Available: SFG time course study of fibrinogen solution contacting PEU and SFG fitting param-

eters of polymers with adsorbed fibrinogen/PBS interfaces after adsorption times from 10−90 min. This material is available free of charge via the Internet at http://pubs.acs.org.

References and Notes

(1) Tang, L.; Eaton, J. W. *Am. J. Clin. Pathol.* **1995**, *103*, 466−471.

(2) Elbert, D. L.; Hubbell, J. A. *Annu. Rev. Mater. Sci.* **1996**, *26*, 365−394.

(3) Wisniewski, N.; Reichert, M. *Colloids Surf., B* **2000**, *18*, 197−219.

(4) Feng, L.; Andrade, J. D. In *Proteins at Interfaces II. Fundamentals and Applications*; Horbett, T. A., Brash, J. L., Eds.; American Chemical Society: Washington, DC, 1995; pp 66−79.

(5) Mosesson, M. W.; Siebenlist, K. R.; Meh, D. A. *Ann. N.Y. Acad. Sci.* **2001**, *936*, 11−30.

(6) Weisel, J. W.; Stauffacher, C. V.; Bullitt, E.; Cohen, C. *Science* **1985**, *230*, 1388−1391.

(7) Hantgan, R. R. *Biochemistry* **1982**, *21*, 1821−1829.

(8) Weisel, J. W.; Medved, L. *Ann. N.Y. Acad. Sci.* **2001**, *936*, 312−327.

(9) O'Connor, S. M.; DeAnglis, A. P.; Gehrke, S. H.; Retzinger, G. S. *Biotechnol. Appl. Biochem.* **2000**, *31*, 185−196.

(10) Tsai, W.; Grunkemeier, J. M.; Horbett, T. A. *J. Biomed. Mater. Res.* **1999**, *44*, 130−139.

(11) Werner, C.; Eichhorn, K.; Grundke, K.; Simon, F.; Grahlert, W.; Jacobasch, H. *Colloids Surf., A* **1999**, *156*, 3−17.

(12) Huang, S.; Ou, C.; Lai, J. *J. Membr. Sci.* **1999**, *161*, 21−29.

(13) Ta, T. C.; Sykes, M. T.; McDermott, M. T. *Langmuir* **1998**, *14*, 2435−2443.

(14) Sit, P. S.; Marchant, R. E. *Thromb. Haemostasis* **1999**, *82*, 1053−1060.

(15) Cacciafesta, P.; Humphris, A. D. L.; Jandt, K. D.; Miles, M. J. *Langmuir* **2000**, *16*, 8167−8175.

(16) Marchin, K. L.; Berrie, C. L. *Langmuir* **2003**, *19*, 9883−9888.

(17) Lenk, T. J.; Horbett, T. A.; Ratner, B. D.; Chittur, K. K. *Langmuir* **1991**, *7*, 1755−1764.

(18) Balasubramanian, V.; Grusin, N. K.; Bucher, R. W.; Turitto, V. T.; Slack, S. M. *J. Biomed. Mater. Res.* **1999**, *44*, 253−260.

(19) Wang, J.; Woodcock, S. E.; Buck, S. M.; Chen, C.; Chen, Z. *J. Am. Chem. Soc.* **2001**, *123*, 9470−9471.

(20) Chen, C.; Wang, J.; Woodcock, S. E.; Chen, Z. *Langmuir* **2002**, *18*, 1302−1309.

(21) Rao, A.; Rangwalla, H.; Varshney, V.; Dhinojwala, A. *Langmuir* **2004**, *20*, 7183−7188.

(22) McGall, S. J.; Davies, P. B.; Neivandt, D. J. *J. Phys. Chem. B* **2004**, *108*, 16030−16039.

(23) Sung, J.; Kim, D.; Whang, C. N.; Ohe, M.; Yokoyama, H. *J. Phys. Chem. B* **2004**, *108*, 10991−10996.

(24) Li, G.; Ye, S.; Morita, S.; Nishida, T.; Osawa, M. *J. Am. Chem. Soc.* **2004**, *126*, 12198−12199.

(25) Liu, Y.; Messmer, M. C. *J. Phys. Chem. B* **2003**, *107*, 9774−9779.

(26) Hong, S.; Zhang, C.; Shen, Y. R. *Appl. Phys. Lett.* **2003**, *82*, 3068−3070.

(27) Wilson, P. T.; Briggman, K. A.; Wallace, W. E.; Stephenson, J. C.; Richter, L. J. *Appl. Phys. Lett.* **2002**, *80*, 3084−3086.

(28) Wang, J.; Buck, S. M.; Chen, Z. *J. Phys. Chem. B* **2002**, *106*, 11666−11672.

(29) Wang, J.; Buck, S. M.; Even, M. A.; Chen, Z. *J. Am. Chem. Soc.* **2002**, *124*, 13302−13305.

(30) Jung, S.; Lim, S.; Albertorio, F.; Kim, G.; Gurau, M. C.; Yang, R. D.; Holden, M. A.; Cremer, P. S. *J. Am. Chem. Soc.* **2003**, *125*, 12782−12786.

(31) Kim, J.; Somorjai, G. A. *J. Am. Chem. Soc.* **2003**, *125*, 3150−3158.

(32) Dreesen, L.; Humbert, C.; Sartenaer, Y.; Caudano, Y.; Volcke, C.; Mani, A. A.; Peremans, A.; Thiry, P. A.; Hanique, S.; Frere, J. *Langmuir* **2004**, *20*, 7201−7207.

(33) Doyle, A. W.; Fick, J.; Himmelhaus, M.; Eck, W.; Graziani, I.; Prudovsky, I.; Grunze, M.; Maciag, T.; Neivandt, D. J. *Langmuir* **2004**, *20*, 8961−8965.

(34) Chen, X.; Clarke, M. L.; Wang, J.; Chen, Z. *Int. J. Mod. Phys. B* **2005**, *20*, 691−713.

(35) Wang, J.; Even, M. A.; Chen, X.; Schmaier, A. H.; Waite, J. H.; Chen, Z. *J. Am. Chem. Soc.* **2003**, *125*, 9914−9915.

(36) Wang, J.; Chen, X.; Clarke, M. L.; Chen, Z. *Proc. Natl. Acad. Sci. U.S.A.* **2005**, *102*, 4978−4983.

(37) Knoesen, A.; Pakalnis, S.; Wang, M.; Wise, W. D.; Lee, N.; Frank, C. W. *IEEE J. Sel. Top. Quantum Electron.* **2004**, *10*, 1154−1163.

(38) Chen, X.; Wang, J.; Sniadecki, J. J.; Even, M. A.; Chen, Z. *Langmuir* **2005**, *21*, 2262−2264.

(39) Perry, A.; Ahlborn, H.; Space, B.; Moore, P. B. *J. Chem. Phys.* **2003**, *118*, 8411−8419

(40) Chen, Z.; Ward, R.; Tian, Y.; Malizia, F.; Gracias, D. H.; Shen, Y. R.; Somorjai, G. A. *J. Biomed. Mater. Res.* **2002**, *62*, 254−264.

(41) Berrocal, M. J.; Badr, I. H. A.; Gao, D. O.; Bachas, L. G. *Anal. Chem.* **2001**, *73*, 5328−5333.

(42) Clarke, M. L.; Wang, J.; Chen, Z. *Anal. Chem.* **2003**, *75*, 3275−3280.

(43) Shen, Y. R. In *The Principles of Nonlinear Optics*; John Wiley & Sons: New York, 1984.

(44) Shen, Y. R. *Annu. Rev. Phys. Chem.* **1989**, *40*, 327−350.

(45) Bain, C. D. *J. Chem. Soc., Faraday Trans.* **1995**, *91*, 1281−1296.

(46) Richmond, G. L. *Chem. Rev.* **2002**, *102*, 2693−2724.

(47) Buck, M.; Himmelhaus, M. *J. Vac. Sci. Technol., A* **2001**, *19*, 2717−2736.

(48) Wang, J.; Chen, C.; Buck, S. M.; Chen, Z. *J. Phys. Chem. B* **2001**, *105*, 12118−12125.

(49) Marx, K. A. *Biomacromolecules* **2003**, *4*, 1099−1120.

(50) Arnau, A.; Sogorb, T.; Jimenez, Y. *Rev. Sci. Instrum.* **2002**, *73*, 2724−2737.

(51) Voinova, M. V.; Jonson, M.; Kasemo, B. *Biosens. Bioelectron.* **2002**, *17*, 835−841.

(52) Hoeoek, F.; Kasemo, B.; Nylander, T.; Fant, C.; Sott, K.; Elwing, H. *Anal. Chem.* **2001**, *73*, 5796−5804.

(53) Sellborn, A.; Andersson, M.; Fant, C.; Gretzer, C.; Elwing, H. *Colloids Surf., B* **2003**, *27*, 295−301.

(54) Voros, J. *Biophys. J.* **2004**, *87*, 553−561.

(55) Sauerbrey, G. *Z. Phys.* **1959**, *155*, 206−222.

(56) Tanaka, M.; Mochizuki, A.; Motomura, T.; Shimura, K.; Onishi, M.; Okahata, Y. *Colloids Surf., A* **2001**, *193*, 145−152.

(57) Lin, T.; Hu, C.; Chou, T. *Biosens. Bioelectron.* **2004**, *20*, 75−81.

(58) McCarthy, S. J.; Meijs, G. F.; Mitchell, N.; Gunatillake, P. A.; Heath, G.; Brandwood, A.; Schindhelm, K. *Biomaterials* **1997**, *18*, 1387−1409.

(59) Schwinte, P.; Voegel, J.; Picart, C.; Haikel, Y.; Schaaf, P.; Szalontai, B. *J. Phys. Chem. B* **2001**, *105*, 11906−11916.

(60) Wang, J.; Paszti, Z.; Even, M. A.; Chen, Z. *J. Phys. Chem. B* **2004**, *108*, 3625−3632

(61) Ostroverkhov, V.; Waychunas, G. A.; Shen, Y. R. *Phys. Rev. Lett.* **2005**, *94*, 046102.

(62) Wang, J.; Chen, X.; Clarke, M. L.; Chen, Z., submitted for publication.